Effect of post-weld heat treatment on joint properties of friction welded joint between brass and low carbon steel

M. Kimura*[1], M. Kusaka[1], K. Kaizu[1] and A. Fuji[2]

This paper describes the effect of post-weld heat treatment (PWHT) on joint properties of copper-zinc alloy (brass) and low carbon steel (LCS) friction welded joints. The as-welded joint obtained 100% joint efficiency and the brass base metal fracture without cracking at the weld interface, and had no intermetallic compound (IMC) layer. The joint efficiency with PWHT decreased with increasing heating temperature and its holding time, and its scatter increased with increasing those parameters. When the joint was heat-treated at 823 K for 360 ks, it did not achieve 100% joint efficiency and fractured between the weld interface and the brass base metal although it had no IMC. The cracking at the peripheral portion of the weld interface was generated through PWHT. The cracking was due to the dezincification and the embrittlement of the brass side during PWHT.

Keywords: Friction welding, Brass, Low carbon steel, Post-weld heat treatment, Joint properties, Crack, Dezincification, Embrittlement

Introduction

Generally speaking, the possibility of generating the intermetallic compound (IMC) for the friction welding method is lower than that of the fusion welding method, since strong plastic flow is produced at the weld interface and its adjacent region during the friction process.[1,2] However, several friction welded joints for dissimilar materials had brittle IMC.[3] Hence, control of the IMC for a dissimilar joint is more important for making a sound joint because the IMC exerts an effect on the joint characteristics. On the other hand, it has been noted that the joint strength was decreased due to generating the IMC by the interdiffusion of both materials used when a sound dissimilar joint with no IMC was used under high temperature.[4-11] That is, it is considered that the IMC is generated at the weld interface of the dissimilar joint by post-weld heat treatment (PWHT) and that affects the joint properties. Hence, a selection guideline for the designs of the dissimilar joint for industrial use is strongly required, although the joint properties of several dissimilar joints improved with PWHT.[10-14] From the viewpoint of scanty generating for the ICM under the conditions of the melting point or lower, it is considered that the dissimilar joint between copper (Cu) or its alloys and steel is useful at relatively high temperature conditions because those combinations had relatively poor interdiffusion.[15] Some researchers have reported that the mechanical and metallurgical properties under the as-welded condition of friction welded joints between Cu or its alloys and steel show desirable characteristics.[16-21] However, the joint properties with PWHT conditions were not investigated.

In previous works,[22,23] the authors clarified the joining phenomena and tensile strength of the friction welded joint between pure Cu or its alloys and steel. The authors also presented the friction welding conditions for the base metal fracture in Cu or its alloys with no cracking at the weld interface. The authors also showed that those joints had no IMC layer. However, the joint properties during PWHT conditions for industrial usages were not investigated. In particular, clarifications of PWHT conditions on the joint properties are strongly required because an expansion in the use of dissimilar friction welded joints is expected.

Based on the above background, the authors have been carrying out research to clarify the joint properties between dissimilar materials during PWHT. In the present work, the authors investigate the effect of PWHT on joint properties of friction welds between a typical Cu alloy, i.e. alpha-beta brass (Muntz metal), and low carbon steel. The authors also show the joint tensile strength under various PWHT conditions and demonstrate the cause of the joint fracture during PWHT.

Experimental procedure

The materials used were alpha-beta brass (referred to as brass) plate with a thickness of 16 mm, and low carbon steel (referred to as LCS) rod with a diameter of 16 mm. The chemical composition of brass was 60.0Cu-40.0Zn in mass%, the ultimate tensile strength was 391 MPa, the 0.2% yield strength was 247 MPa, and the elongation was 46%. The chemical composition of LCS was 0.16C-0.45Mn-0.20Si-0.12P-0.18S in mass%, the ultimate tensile

[1]Department of Mechanical and System Engineering, Graduate School of Engineering, University of Hyogo, 2167 Shosha, Himeji, Hyogo 671-2280, Japan
[2]Department of Mechanical Engineering, National University Corporation–Kitami Institute of Technology, 165 Koen-cho, Kitami, Hokkaido, 090-8507, Japan

*Corresponding author, email mkimura@eng.u-hyogo.ac.jp

strength was 451 MPa, the yield strength was 284 MPa, and the elongation was 36%. The brass plate was cut in a rectangular shape along the rolling direction, and then machined to a 12 mm diameter for the weld faying (contacting) surface. The LCS rod was also machined to a 12 mm diameter for the weld faying surface. All weld faying surfaces of specimens were polished with a surface grinding machine before joining in order to eliminate the effect of surface roughness on the mechanical properties of joints. The materials used and specimen shapes were identical to those in a previous report.[23]

A continuous (direct) drive friction welding machine, which had an electromagnetic clutch in order to prevent braking deformation during the rotation stop, was used for the joining. During the friction welding operations, the friction welding condition was set to the following combinations: a friction speed of 27.5 s^{-1} (1650 rpm), a friction pressure of 90 MPa, a friction time of 1.5 s, a forge pressure of 90 MPa, and a forge time of 6.0 s. The details of the joining method have been previously described,[24,25] and the friction welding condition was also determined in the previous report.[23] That is, when the joint was made with this condition, it had the tensile strength of the brass base metal and the brass base metal fracture with no cracking at the weld interface. In addition, this joint had no IMC layer. The details of the joint characteristics have been also previously described.[23] All joint tensile test specimens were machined to 12 mm in diameter and 84 mm in parallel length. Following the mechanical processing operation, the joint was heat treated in a vacuum environment of approximately 0.1 Pa (7.5×10^{-4} torr) at heating temperatures of 623, 723, and 823 K (350, 450, and 550 ℃) for holding times of 3.6, 36, and 360 ks (1, 10, and 100 hours). A heating temperature of 623 K was set, and that was higher than the stress-relieving temperature and lower than the annealing temperature.[26] Also, the heating temperatures of 723 and 823 K were set within the annealing temperature.[26] The heating rate during PWHT was 2 Ks^{-1} and all joints were immediately air cooled at a room temperature following known holding times. After the PWHT operation, a joint tensile test was carried out at room temperature. Analysis via EDS was carried out to analyze the chemical composition in the weld interface region.

Results

Joint tensile strength

Figure 1 shows the relationship between the heating temperature and the joint efficiency. The joint efficiency was defined as the ratio of joint tensile strength of the PWHT joint to the ultimate tensile strength of the brass base metal that was treated with the same PWHT conditions. Figure 2 shows the examples of the appearances of joint tensile test specimens after tensile testing. The as-welded joint had 100% joint efficiency and

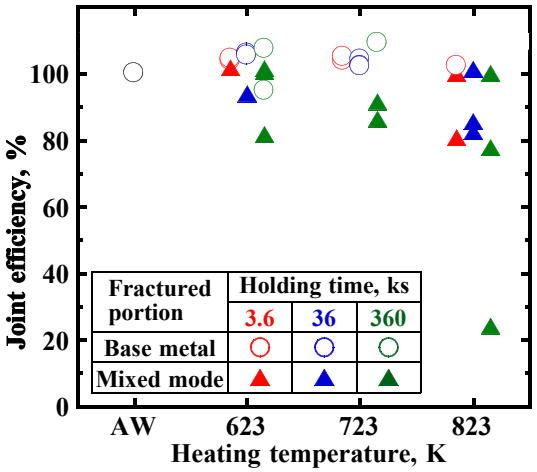

1 Relationship between heating temperature and joint efficiency

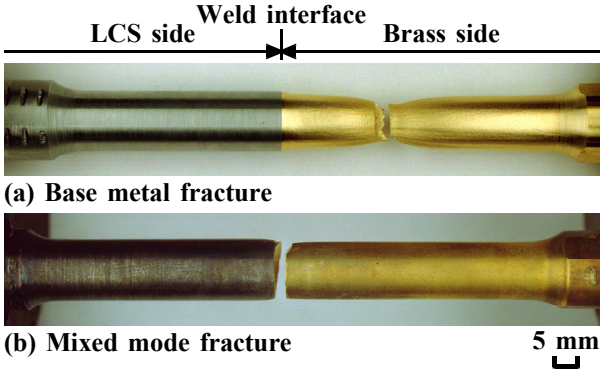

2 Examples of appearances of joint tensile test specimens after tensile testing

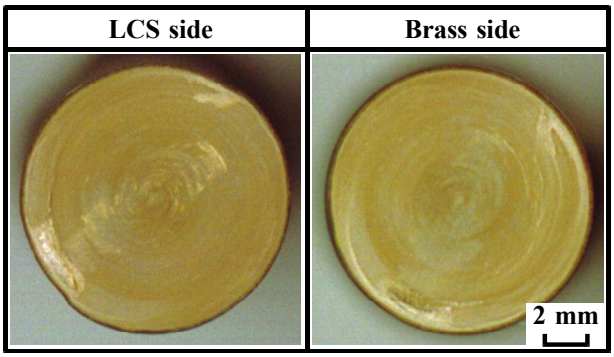

3 Example of frctured surface with mixed mode fracture of joint tensile test specimens after tensile testing

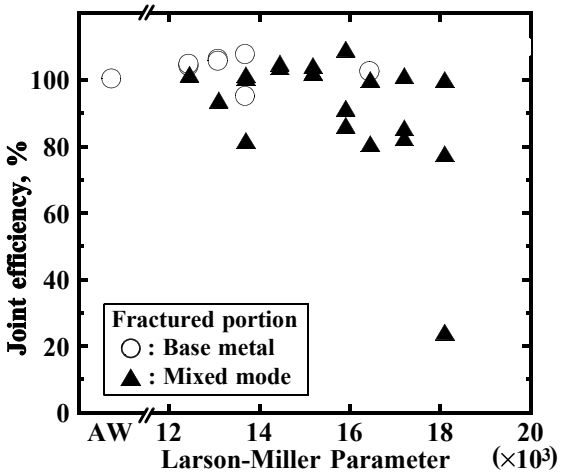

4 Relationship between Larson-Miller parameter and joint efficiency

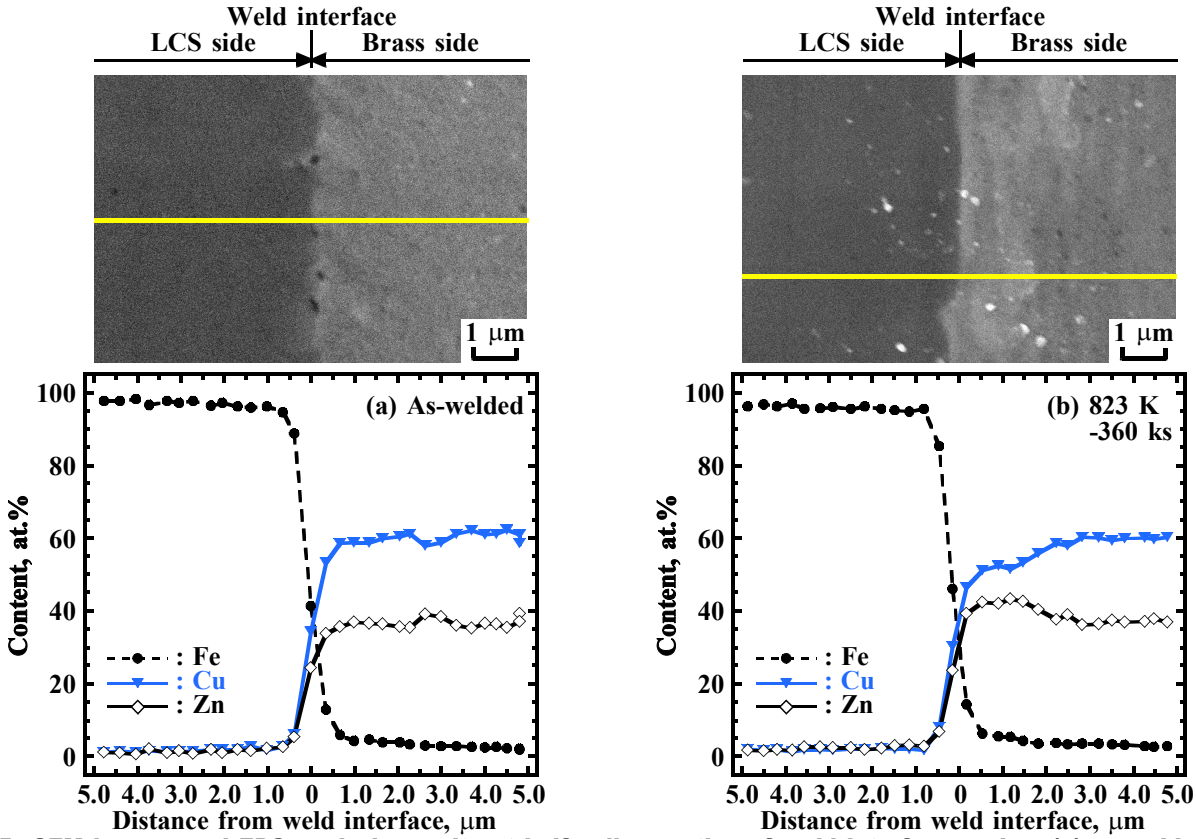

5 SEM images and EDS analysis results at half-radius portion of weld interface region; (a) as-welded joint, (b) PWHT joint with 823 K -360 ks

the brass base metal fracture with no cracking at the weld interface, as shown in Fig. 2a. However, the joint efficiency decreased with increasing heating temperature and its holding time (see Fig. 1). Moreover, the scatter of the joint efficiency increased with the increase of those PWHT parameters. Several PWHT joints with the base metal fracture had cracking at the weld interface. When the joint was heat-treated at 823 K for 36 ks or longer, all joints were fractured between the weld interface and the brass base metal (referred to as mixed mode fracture), as shown in Fig. 2b. The fractured surfaces as shown in Fig. 3 demonstrated a relatively flat plane in comparison with that of the as-welded joint.[23] That is, the roughness of the fractured surfaces was small. Figure 4 shows the relationship between the Larson-Miller parameter (LMP)[27] and the joint efficiency. LMP was defined as shown in following equation:

$$LMP = T\left(\log_{10} t + 20\right) \quad (1)$$

where T is heating temperature [K] and t is PWHT holding time [h]. The joint efficiency decreased with increasing LMP value. In particular, almost all joints had the mixed mode fracture when the LMP value was larger than approximately 14,000. That is, the fact that the joint efficiency was decreased was due to PWHT for the joint.

Observation of weld interface region

Figure 5 shows the SEM images and EDS analysis results at the half-radius portion of the weld interface region for the joints. One of the joints was the as-welded joint, and the other one was the PWHT joint which was heat-treated at 823 K for 360 ks. The weld interface of the as-welded

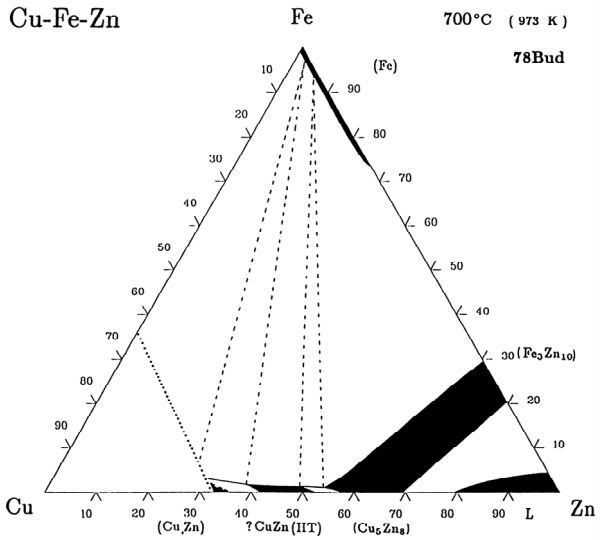

6 Ternary alloy phase diagram of Cu, Fe and Zn at temperature of 923 K[28]

joint was clear, and the distribution lines corresponding to Cu, Fe, and Zn by EDS analysis had no plateau part at the weld interface (Fig. 5a). The weld interface of the PWHT joint was also clear and the distribution lines had no plateau part, although Zn content at the adjacent region of the weld interface on the brass side of it was a little higher than that of the as-welded joint (Fig. 5b). Other PWHT joints also did not have the IMC layer, based on the SEM observation level, although that data was not shown due to space limitations. That is, even if the joint

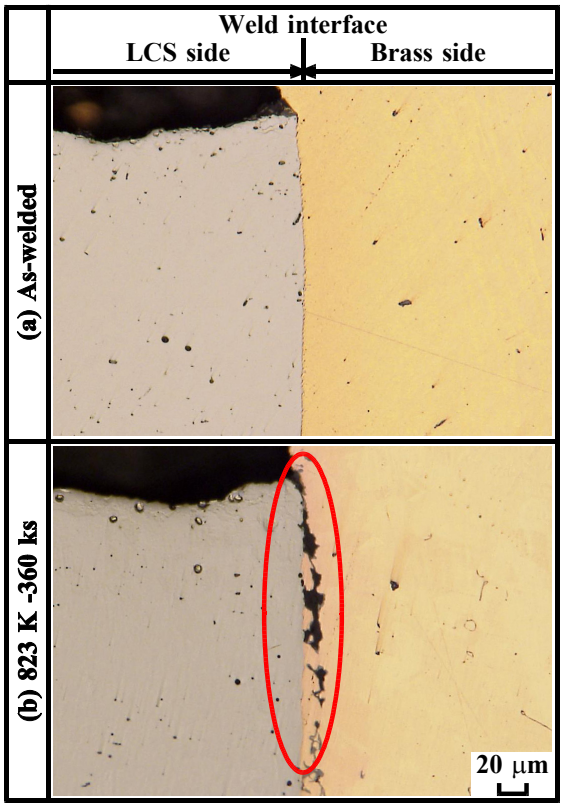

7 Cross-sectional appearances of weld interface region; (a) as-welded joint, (b) PWHT joint with 823 K -360 ks

was treated with PWHT, an IMC layer was not observed. Figure 6 shows the ternary alloy phase diagram of Cu, Fe and Zn at temperature of 923 K (700 ℃).[28] The IMC layer was not easily formed at this temperature. The welding and PWHT temperatures were lower than that of this temperature. Therefore, this result also suggested that the IMC layer was difficult to generate from the ternary alloy phase diagram with the material combination in this study.

Figure 7 shows the cross-sectional appearances of the weld interface region for the as-welded and PWHT joints. The as-welded joint had no defect at the weld interface, as shown in Fig. 7a. However, the PWHT joint had defects such as the cracking at the peripheral portion of the weld interface indicated by the ellipse in Fig. 7b. The crack length increased with increasing heating temperature and its holding time. Hence, the cracking by PWHT seems to be a cause of the decrease of the joint efficiency.

Observation of fractured surface

Figure 8 shows the fractured surfaces at the peripheral portion of the LCS side for joints with the mixed mode fracture after tensile testing. The peripheral portion at the fractured surfaces of the joint, which was heat-treated at 623 K for 360 ks, had a slight flat plane from the outer surface to the centre axis direction, as shown in Fig. 8a. When the joint was heat-treated at 723 or 823 K for 360 ks, the peripheral portion of the fractured surfaces also had the flat plane (see Figs. 8b and 8c). The area of the flat plane at the peripheral portion increased with increasing heating temperature and its holding time. In addition, this flat plane was slightly rough compared with the other part of the fractured surface. All of the other PWHT joints with the mixed mode fracture had the flat plane. Thus, the decline of the joint efficiency with PWHT was due to a cracking during PWHT.

Figure 9 shows the SEM micrographs of fractured surfaces at the half-radius portion of the LCS side for joints with the mixed mode fracture after tensile testing, corresponding to the results of the brass base metal. In this case, the tensile test of the brass base metal was carried out after PWHT operation, which was treated with the same PWHT condition for the PWHT joint. All fractured surfaces of the brass base metal had a dimple pattern. Thus, the fracture of the brass base metal was a typical ductile fracture. On the other hand, the fractured surfaces of the joint, which was heat-treated at 723 and 823 K for 360 ks, did not have a dimple surface although that at 623 K for 360 ks had a dimple pattern similar to the brass base metal. That is, the fracture of the joint at a heating temperature of 723 K or over was a typical brittle fracture. Therefore, the decreasing joint efficiency was due to the embrittlement at the weld interface of the brass side.

Investigation of weld interface fracture result

Since it was considered that the cracking was generated at the weld interface during the air cooling after PWHT due to the difference of the coefficient of linear expansion between materials used, the effect of the cooling speed on

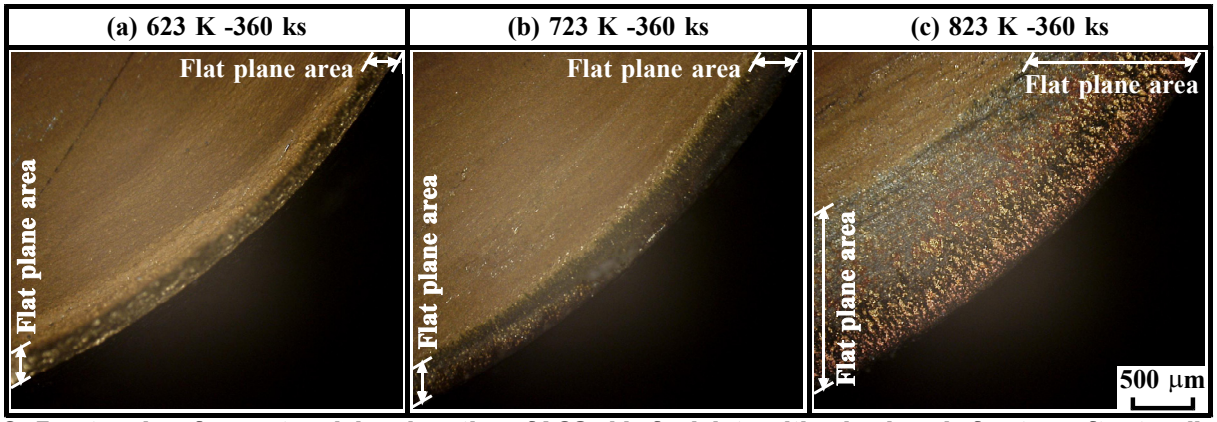

8 Fractured surfaces at peripheral portion of LCS side for joints with mixed mode fracture after tensile testing; (a) 623 K -360 ks, (b) 723 K -360 ks, and (c) 823 K -360 ks

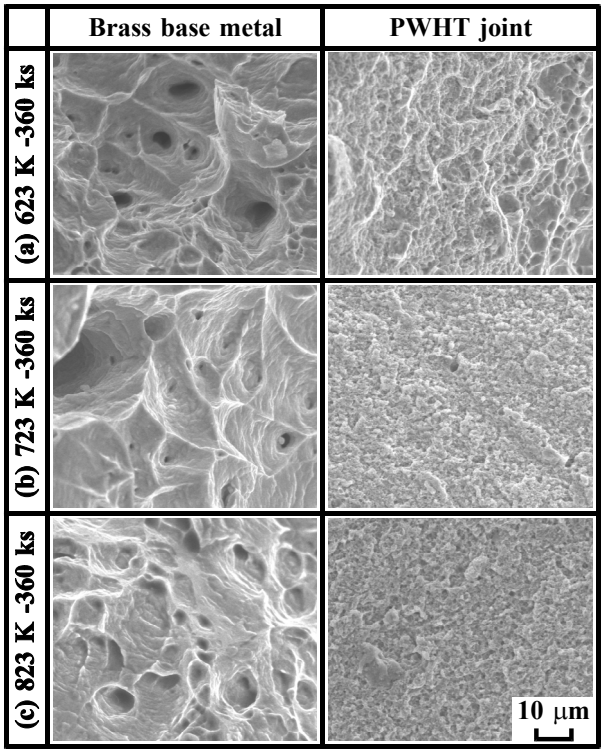

9 SEM micrographs of fractured surfaces at half-radius portion of LCS side for joints with mixed mode fracture after tensile testing, corresponding to those result of brass base metal ; (a) 623 K -360 ks, (b) 723 K -360 ks, and (c) 823 K -360 ks

joint properties was investigated. Table 1 summarises the results of tensile test of joints at various cooling processes that were heat-treated at 723 K for 360 ks. In this case, the cooling time of furnace cooling from PWHT temperature until room temperature was about 2 days. The tensile strength and joint efficiency of the joint with furnace cooling were similar to that with air cooling. That is, the joint with furnace cooling did not achieve 100% joint efficiency, and all joints had the mixed mode fracture. Also, the cross-section of the joint with furnace cooling had cracking at the weld interface. Therefore, it was clarified that the cracking at the weld interface of the joint was generated during PWHT. The cracking at the peripheral portion of the weld interface seems to be a cause of the difference of the coefficient of linear expansion between the brass and LCS.

To remove the cracking at the weld interface of the joint, a joint tensile test was carried out with a specimen with 9 mm in diameter at the parallel part because the maximum crack length was approximately 0.5 mm from the outer surface of the joint in this experiment. Table 2 summarises the results of tensile test specimens with various diameter that were heat-treated at 823 K for 360 ks. In this case, joints were treated with air cooling, and the joint tensile test specimen was machined after PWHT. The joint with 9 mm in diameter at the parallel part also did not achieve 100% joint efficiency, and all joints had the mixed mode fracture. Moreover, the fractured surface was similar to the joint with 12 mm in diameter. Hence, it is considered that the joint did not achieve 100% joint efficiency due to the embrittlement at the weld interface

Table 1 Results of tensile test of joints at various cooling processes for joints with 723 K -360 ks

Cooling method	Tensile strength, MPa		Joint efficiency, %	
	Range	Average	Range	Average
Air cooling	271-343	301	86.0-108.9	95.5
Furnace cooling	267-316	287	84.8-100.3	91.2

Table 2 Results of tensile test specimens with various diameter for joints with 823 K -360 ks

Specimen diameter, mm	Tensile strength, MPa		Joint efficiency, %	
	Range	Average	Range	Average
12	65-270	182	24.0-99.6	67.0
9	66-167	117	24.4-61.6	43.2

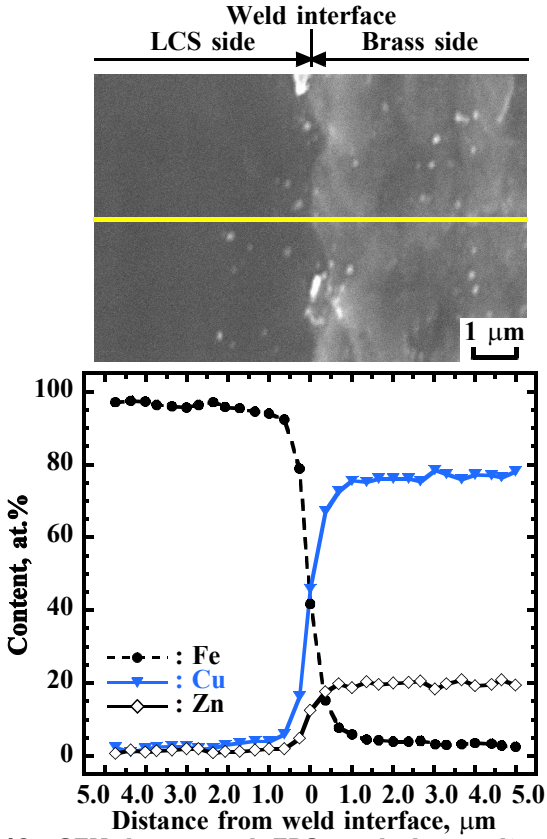

10 SEM image and EDS analysis result at peripheral portion of weld interface region of joint with 823 K -360 ks

of the brass side.

Figure 10 shows the SEM image and EDS analysis result at the peripheral portion of the weld interface region of the joint, which were heat-treated at 823 K for 360 ks. In this case, the peripheral portion of the joint showed the opposite of that in Fig. 7b. The distribution lines corresponding to Cu, Fe, and Zn by EDS analysis had no plateau part. Hence, the joint also had no IMC layer at the peripheral portion. However, Zn content was lower than that of the half-radius portion (see Fig. 5b).

That is, Zn content differed in the measuring portion although the observed joint was the same. In addition, the ratio of Zn content to Cu content at the peripheral portion was decreased to about 60% in comparison with that of the as-welded joint. That is, Zn content at the peripheral portion of the brass side was vaporized in a vacuum from the peripheral surface of it, although that at the other portions was hardly vaporized because those portion was not adjacent to the peripheral surface. Therefore, it was clarified that the Zn content of the brass base metal at this region was decreased by PWHT.

Discussion

Based on the above results, the fact of the decline in joint properties by PWHT was considered as follows. The Zn in the brass was vaporized in a vacuum, and its volume increased with increasing heating temperature and its holding time.[29-32] Moreover, the body volume of the brass was constricted by vaporization of Zn during heat treatment.[33-37] It is considered that the constricted body volume of the brass increased with increasing heating temperature and its holding time, and the decreasing joint efficiency through PWHT was due to the dezincification and constriction of the brass side. That is, the body volume of the brass side will be constricted by vaporization of Zn in a vacuum, and also the cracks will be generated at the weld interface by the difference of the coefficient of linear expansion between the brass and LCS. If the mixed mode fracture of the joint was produced by only cracking, that should be a fracture at the brass base metal. However, the joint with 9 mm in diameter at the parallel part of the tensile specimen did not achieve 100% joint efficiency, and it had the mixed mode fracture (see Table 2). Therefore, another factor seems to be the cause of the mixed mode fracture for the joint. On the other hand, it is considered that the brass with high residual stress easily became embrittled due to the growth of the intercrystalline void and the grain size of the brass.[38-40] In addition, the residual stress adjacent region of the weld interface will be able to be estimated as higher than that of the other part, and which result was also described in some reports.[41-45] That is, it is considered that the susceptibility of embrittlement of the adjacent region at the weld interface for the PWHT joint is high. Consequently, the PWHT joint had the brittle fracture of the brass side at the weld interface, although it was annealed (see Fig. 8). The fact that the joint efficiency was decreased by PWHT was due to the dezincification and embrittlement of the brass side during PWHT, although further investigation is necessary to elucidate the detailed the joint properties. Thus, the joint between brass and LCS should not be used under high temperature conditions.

Conclusions

This report described the effect of post-weld heat treatment (PWHT) on joint properties of copper-zinc alloy (brass) and low carbon steel (LCS) friction welded joints. In particular, we investigated the joint tensile strength under various PWHT conditions, and the cause of the joint fracture during PWHT. The following conclusions are provided.

1. The as-welded joint was made through a friction speed of 27.5 s^{-1}, a friction pressure of 90 MPa, a friction time of 1.5 s, a forge pressure of 90 MPa, and a forge time of 6.0 s. This joint had 100% joint efficiency and a brass base metal fracture with no cracking at the weld interface. In addition, the as-welded joint had no intermetallic compound (IMC) layer at the weld interface, which was based on the SEM observation level.
2. The joint efficiency decreased with increasing heating temperature and its holding time. Moreover, the scatter of the joint efficiency increased with increasing those PWHT parameters. When the joint was heat-treated at 823 K for 36 ks or longer, all joints were fractured between the weld interface and the brass base metal.
3. The PWHT joint had defects such as cracking at the peripheral portion of the weld interface, although it did not have the IMC layer based on the SEM observation level. In addition, the PWHT joint at a heating temperature of 723 K or over had a typical brittle fracture.
4. Zn content at the peripheral portion of the PWHT joint was lower than that of the half-radius portion. In addition, the ratio of Zn content to Cu content at the peripheral portion was decreased to about 60% in comparison with that of the as-welded joint.
5. The cracking was due to the dezincification and embrittlement of the brass side during PWHT.

In conclusion, a joint between brass and LCS should not be used under high temperature conditions.

Acknowledgements

This research was partially supported by the Ministry of Education, Culture Sports, Science and Technology, Grant-in-Aid for Young Scientists (B), 20760496, 2008. We wish to thank the staff members of the Machine and Workshop Engineering at the Graduate School of Engineering, University of Hyogo. We also wish to thank the alumnus Mr Masanori Tabayashi in Himeji Institute of Technology (present, University of Hyogo) for his devoted contributions to this research project. Also, we wish to thank Mr Hideaki Tohkuni in National University Corporation-Kitami Institute of Technology for his kindly and aggressive assisting to this study.

References

1. K. K. Wang: *Welding Research Council Bulletins*, 1975, WRC Bulletin 204, 1-21.
2. Japan Friction Welding Association: "Friction Welding", 6-14; 1979, Tokyo, Corona Publishing (in Japanese).
3. Americaan Welding Society: "WELDING HANDBOOK, Eighth Edition, Vol. 2", 750-755; 1991, Miami, FL, Americaan Welding Society.
4. K. G. K. Murti and S. Sundaresan: *Weld. J.*, 1985, **64**, 327s-334s.
5. A. Fuji, K. Ameyama, M. Futamata and Y. Shimaki: *Q. J. Jpn. Weld. Soc*., 1994, **12**, (1), 101-107 (in Japanese).
6. A. Fuji, K. Ameyama and T. H. North: *J. Mater. Sci.*, 1995, **30**, (20), 5185-5191.
7. T. Ohnishi, K. Yasumi, K. Ogawa, H. Tsubakino, A. Yamamoto and H. Ochi: *J. Jpn. Inst. Light Met.*, 1996, **46**, (12), 619-625 (in Japanese).
8. A. Fuji, T. Nagano, Y. C. Kim and J. Yan: *J. Light Metal Welding & Construction*, 2007, **45**, (7), 333-345 (in Japanese).
9. M. Kimura, H. Ishii, M. Kusaka, K. Kaizu and A. Fuji: *Sci. Technol. Weld. Joining*, 2009, **14**, (5), 388-395.
10. A. Fuji, T. H. North, K. Ameyama and M. Futamata: *Mater. Sci.*

Technol., 1992, **8**, (3), 219-235.
11. A. Fuji, Y. Horiuchi and K. Yamamoto: *Sci. Technol. Weld. Joining*, 2005, **10**, (3), 287-294.
12. A. Fuji, K. Ameyama and T. H. North: *J. Mater. Sci.*, 1996, **31**, (3), 819-827.
13. H. Ochi, K. Ogawa, Y. Yamamoto and Y. Suga: *J. Jpn. Soc. Fract. Strength Mater.*, 1998, **32**, (2), 43-50 (in Japanese).
14. A. Fuji, K. Ikeuchi, Y. S. Sato and H. Kokawa: *Sci. Technol. Weld. Joining*, 2004, **9**, (6), 507-512.
15. Japan Institute of Metals: "Data Book of Metals, Fourth revision", 20-25; 2008, Tokyo, Maruzen (in Japanese).
16. A. Z. Sahin, B. S. Yibaş, M. Ahmed and J. Nickel: *J. Mater. Process. Technol.*, 1998, **82**, 127-136.
17. K. Tsuchiya and H. Kawamura: *J. Nucl. Mater.*, 1996, **233**/**237**, 913-917.
18. H. Yamaguchi, K. Ogawa, H. Ochi, T. Sawai, G. Kawai, Y. Yamamoto and R. Tsujino: *J. Jpn. Res. Inst. Adv. Copper-Base Mater. and Technol.*, 2003, **42**, (1), 132-136 (in Japanese).
19. W. B. Lee and S. B. Jung: *Z. Metallku.*, 2003, **94**, (12), 1300-1306.
20. G. Kawai, H. Ochi, R. Tsujino, H. Yamaguchi, Y. Yamamoto and K. Ogawa: *J. High Press. Inst. Jpn.*, 2004, **42**, (4), 199-206 (in Japanese).
21. G. Kawai, H. Ochi, H Yamaguchi and K. Sakurai, K.: *J. Jpn. Res. Inst. Adv. Copper-Base Mater. and Technol.*, 2005, **44**, (1), 248-252 (in Japanese).
22. M. Kimura, M. Kusaka, K. Kaizu and A. Fuji: *J. Solid Mech. Mater. Eng.*, 2009, **3**, (2), 187-198.
23. M. Kimura, M. Kusaka, K. Kaizu and A. Fuji: *Sci. Technol. Weld. Joining*, 2009, **14**, (5), 404-412.
24. M. Kimura, M. Choji, M. Kusaka, K. Seo and A. Fuji: *Sci. Technol. Weld. Joining*, 2006, **11**, (2), 209-215.
25. M. Kimura, M. Kusaka, K. Seo and Y. Muramatsu: *Sci. Technol. Weld. Joining*, 2006, **11**, (4), 448-454.
26. Japan Copper and Brass Association: "Data Book of Copper and Brass, Second Edition", 19-20; 2009, Tokyo, Japan Copper and Brass Association (in Japanese).
27. F. R. Larson and A. A. Miller: *Trans. Am. Soc. Mech. Eng.*, 1952, **74**, (7), 765-775.
28. P. Villars, A. Prince and H. Okamoto: in "Handbook of Ternary Alloy Phase Diagrams, Vol. 7", (ed. American Society for Metals), 9462-9469; 1995, Materials Park, OH, American Society for Metals.
29. K. Nagasaki, S. Haruyama, M. Kaneko and I. Itoh: *J. Jpn. Inst. Met.*, 1969, **33**, (11), 1218-1224 (in Japanese).
30. I. Itoh, M. Togashi and T. Hikage: *J. Jpn. Inst. Met.*, 1974, **38**, (4), 294-300 (in Japanese).
31. Y. Taga and K. Nakajima: *J. Jpn. Inst. Met.*, 1976, **40**, (5), 487-491 (in Japanese).
32. K. Asami: *Trans. Jpn. Inst. Met.*, 1980, **21**, (5), 302-308.
33. P. A. Jacquet: *Acta Metall.*, 1954, **2**, (11), 752-769 (in French).
34. N. Brown: *Acta Metall.*, 1959, **7**, (3), 210-215.
35. H. Yamaguchi: *Oyo Buturi*, 1963, **32**, (12), 911-919 (in Japanese).
36. H. Yamaguchi: *Oyo Buturi*, 1964, **33**, (3), 171-181 (in Japanese).
37. F. W. Giacobbe: *J. Alloy Compd.*, 1993, **202**, (1-2), 243-250.
38. S. Sato : *J. Jpn. Inst. Met.*, 1965, **29**, (1), 41-47 (in Japanese).
39. J. D. Wolley and A. G. Fox: *J. Mater. Sci. Lett.*, 1988, **7**, (7), 763-765.
40. B. P. Kashyap, S. Verma, P. Mandlik, N. Kumar and S. P. Toppo: *Mater. Sci. Technol.*, 2006, **22**, (3), 363-367.
41. Y. C. Kim, A. Fuji and T. H. North: *Q. J. Jpn. Weld. Soc*., 1994, **12**, (2), 243-248 (in Japanese).
42. Y. C. Kim, A. Fuji and T. H. North: *Mater. Sci. Technol.*, 1995, **11**, (4), 383-388.
43. A. Fuji, H. Kokawa and Y. C. Kim : *Q. J. Jpn. Weld. Soc*., 2000, **18**, (4), 617-627 (in Japanese).
44. Y. C. Kim and A. Fuji: *Sci. Technol. Weld. Joining*, 2002, **7**, (3), 149-154.
45. Y. Fukuchi and K. Okita: *Trans. Jpn. Soc. Mech. Eng. (Series A)*, 1996, **62**, (599), 1677-1683 (in Japanese).